

## Overview of the FTU results

F. ALLADIO, B. ANGELINI, M.L. APICELLA, G. APRUZZESE, E. BARBATO, L. BERTALOT, A. BERTOCCHI, G. BRACCO, A. BRUSCHI<sup>1</sup>, G. BUCETI, P. BURATTI, A. CARDINALI, S. CASCINO<sup>2</sup>, C. CASTALDO, C. CENTIOLI, R. CESARIO, P. CHUILON, S. CIATTAGLIA, S. CIRANT<sup>1</sup>, V. COCILOVO, F. CRISANTI, R. DE ANGELIS, M. DE BENEDETTI, E DE LA LUNA<sup>3</sup> G. GIRUZZI<sup>4</sup>, F. DE MARCO, B. ESPOSITO, M. FINKENTHAL<sup>5</sup>, B. FRANCONI<sup>2</sup>, D. FRIGIONE, L. GABELLIERI, F. GANDINI<sup>1</sup>, G. GATTI, E. GIOVANNOZZI, C. GORMEZANO, F. GRAVANTI, G. GRANUCCI<sup>1</sup>, M. GROLLI, F. IANNONE, V. KRIVENSKI<sup>3</sup>, H. KROEGLER, E. LAZZARO<sup>1</sup>, M. LEIGHEB, G. MADDALUNO, G. MAFFIA, M. MARINUCCI, G. MAZZITELLI, M. MAY<sup>5</sup>, P. MICOZZI, F. MIRIZZI, S. NOWAK<sup>1</sup>, F.P. ORSITTO, D. PACELLA, L. PANACCIONE, M. PANELLA, P. PAPITTO, V. PERICOLI-RIDOLFINI, A. A. PETROV<sup>6</sup>, L. PIERONI, S. PODDA, F. POLI<sup>2</sup>, G. PUCELLA<sup>2</sup>, G. RAVERA, G.B. RIGHETTI, F. ROMANELLI, M. ROMANELLI, A. RUSSO<sup>2</sup>, F. SANTINI, M. SASSI, S.E. SEGRE<sup>7</sup>, A.SIMONETTO<sup>1</sup>, P. SMEULDERS, E. STERNINI, C. SOZZI<sup>1</sup>, N. TARTONI, B. TILIA, P. E. TREVISANUTTO<sup>2</sup>, A. A. TUCCILLO, O. TUDISCO, V. VERSHKOV<sup>8</sup>, V. VITALE, G. VLAD, V. ZANZA, M. ZERBINI, F. ZONCA

Associazione EURATOM-ENEA sulla Fusione  
C.R. Frascati, 00044, Frascati, Roma, Italy  
e-mail contact of main author: romanelli@frascati.enea.it

**Abstract.** An overview of the FTU results during the period 1998-2000 is presented. FTU has operated up to the nominal parameters ( $B=8T$ ,  $I=1.6MA$ ) with good reliability. Using the high-speed, multiple pellet injection system in 8T/1.25MA discharges a phase lasting a few energy confinement time has been achieved with improved confinement properties with peaked density profiles ( $n=4\times 10^{20}m^{-3}$ ),  $T_e$ ,  $T_i$  and  $Z_{eff}$  1.3. Up to 14 keV of electron temperature have been obtained at high density using electron cyclotron resonance heating (ECRH) on the current ramp. The transport analysis shows a very low electron heat transport in the region with flat/hollow safety factor profile. Synergy studies have been performed with simultaneous injection of lower hybrid and electron cyclotron waves in 7.2T discharges, well above the ECRH resonance. Clear evidence has been obtained of electron cyclotron wave absorption by the lower hybrid produced electron tails. Stabilisation of  $m=2$  tearing modes has been obtained using ECRH, with subsequent improvement of the energy confinement. Ion Bernstein wave injection in high magnetic field ( $B=8T$ ) plasmas has shown the reduction of the electron thermal conductivity in the region inside the absorption radius possibly due to the formation of an internal transport barrier.

## 1. Introduction

Compact, high magnetic field tokamaks have the advantage of producing thermonuclear grade plasmas at high plasma density, low impurity concentration and strong electron-ion

---

<sup>1</sup> Associazione EURATOM-ENEA-CNR sulla Fusione Milano, Ist. Di Fisica del Plasma, Italy

<sup>2</sup> ENEA fellow

<sup>3</sup> CIEMAT, Madrid, Spain

<sup>4</sup> CEA, Cadarache, France

<sup>5</sup> John Hopkins University, Baltimore, USA

<sup>6</sup> State Research Center of Russian Federation, Troitsk Institute for Innovation and Fusion Research, SRC RF TRINITI, Troitsk, Moskow region, 142190 Russia

<sup>7</sup> Dipartimento di Fisica, II Università di Roma "Tor Vergata", Roma Italy

<sup>8</sup> Kurchatov Institute, Moskow, Russian federation

equipartition. The Frascati Tokamak Upgrade (FTU) ( $a=0.3\text{m}$ ,  $R=0.93\text{m}$ ) can exploit these features by working up to a magnetic field  $B=8\text{T}$  and a plasma current  $I=1.6\text{MA}$ . During the last campaign, FTU has been operated up to the nominal parameters with good reliability, avoiding light-impurity contamination problem. Furthermore, the shot by shot use of the titanisation system has been fundamental to obtain high performance discharges. Pellet injection in these conditions allows a substantial increase of the energy confinement time ( $\tau_E = H \times \tau_{E10}$ , with  $H = 1.4-1.7$ ) as long as deep fuelling condition are obtained. A maximum  $n_{e0} \tau_{E10}$  in the range  $n_{e0} \tau_{E10} = 10^{20}\text{m}^{-3}$  has been achieved in  $8\text{T}$ ,  $1.25\text{MA}$ , pellet fuelled, ohmic discharges with low impurity content ( $Z_{\text{eff}} = 1.3$ ) and strong electron-ion equipartition.

Full exploitation of the various heating systems has been made. The Lower Hybrid system ( $8\text{GHz}$ ,  $t_{\text{pulse}}=1\text{s}$ ) is composed by 5 gyrotrons ( $1\text{MW}$  each at the generator) feeding 5 grills on two FTU windows. One of the two Lower Hybrid structures showed a severe leak problem and was dismantled during 1999, reducing the power available to about  $1\text{MW}$  at the plasma, a value which has been routinely achieved during the last campaign. The ECRH system [1] ( $140\text{GHz}$ ,  $t_{\text{pulse}}=0.5\text{s}$ ) has been working at a maximum power level of about  $1.1\text{MW}$  at the plasma (corresponding to three gyrotrons), making use of the launching system capability of injecting power at oblique angle with Current Drive (ECCD) capability. The system has been employed both for transport studies and MHD mode stabilisation. Using ECRH on the current ramp, a central temperature of  $14\text{keV}$  has been achieved at high central plasma density. Simultaneous pellet injection and ECRH has produced improved confinement phases. Stabilisation of  $m=2$  tearing modes by ECRH/ECCD has produced a substantial confinement increase. Furthermore, combined injection of lower hybrid and electron cyclotron waves in  $B=7.2\text{T}$  discharges has produced the first clear sign of synergy between the two waves, with an increase of the order of  $1\text{keV}$  of the electron temperature at the injection of electron cyclotron waves. The Ion Bernstein Wave (IBW) Heating system ( $433\text{MHz}$ ,  $t_{\text{pulse}}=1\text{s}$ ), presently fed by one klystron ( $0.35\text{MW}$  at the plasma), has been employed in high magnetic field discharges (up to  $8.2\text{T}$ , beyond the FTU design value) to investigate the formation of RF-induced sheared flows. Possible evidence of a transport barrier formation are reported in this paper.

## 2. Steady Improved confinement at high density high magnetic field

Use of pellet injection in conditions where injected particles can be ionised close to the plasma centre can lead to plasmas with improved confinement as observed in several experiments [2-6]. Improved confinement is attributed to steep pressure profiles and is called the PEP mode (Pellet Enhanced Performance) but this improved confinement phase does not last very long due to the rapid decay of the pressure gradients. In other experiments, such as ASDEX-U[5], multiple pellets have been used to increase and to maintain high-density plasmas but typically without deep penetration. Multiple deep pellet injection has been used in FTU in order to benefit from the high field capability of the device, hence high density operation, and the availability of a multiple fast pellet injector (up to 8 pellets at  $1.3\text{ km/s}$ ).

In previous FTU experiments[6], improved confinement was achieved in the second pellet phase with the following target plasma parameters: line average density  $n = 1.5 \times 10^{20}\text{m}^{-3}$ ,  $T_{e0} = 1.5\text{ keV}$ ,  $B=7.1\text{T}$  and  $I=0.8\text{MA}$ . Following the second pellet launch, central density was up to  $7 \times 10^{20}\text{m}^{-3}$  and neutron yield up to  $4 \times 10^{12}\text{ n/sec}$ . Transport analysis has indicated that ion diffusivity was neo-classical. These high performance plasmas are very sensitive to  $m=1$  internal kink modes, which can grow to a large amplitude and couple, in some case, to more

external modes, leading to mode-locking and disruptions. In the present campaign, technical availability of FTU has been extended up to 8T, 1.6 MA plasmas with a significant length of the current plateau (0.6 s at 1.6 MA).

The enhanced confinement regimes have been extended up to B=8T, I=1.25MA with multiple pellet injection, only limited by the availability of pellets and the time duration of the current plateau. Disruptions were avoided by careful conditioning of the first wall (using titanisation) and adjusting the target plasma density so as to allow good pellet penetration. Time interval between pellets was selected to be 100 ms, about one energy confinement time.

As shown in Fig1, the best confinement was achieved during the last sequence of pellets.

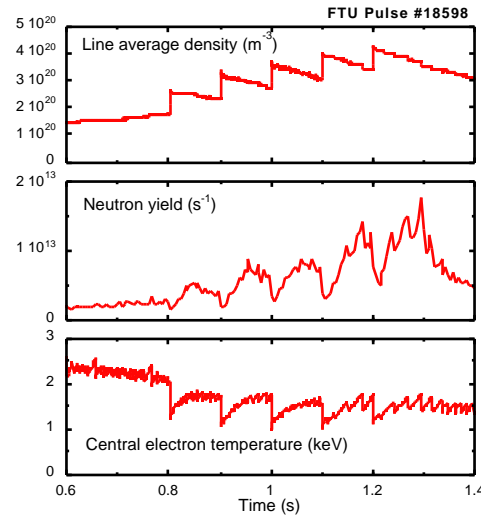


FIG.1 Time traces of line-average density, central electron temperature and neutron yield for FTU pulse #18598, with five pellets injected during the 1.2 MA current plateau at B=8 T (edge safety factor  $q=3.3$ ).

Quasi steady conditions were achieved with a thermal neutron rate up to  $1.8 \times 10^{13}$  n/s, a line averaged density of  $4 \times 10^{20} \text{ m}^{-3}$  (peaked density is estimated to be larger than  $8 \times 10^{20} \text{ m}^{-3}$ ) and central temperature of 1.5 keV. Core transport analysis shows that, in the post-pellet phase, the electron thermal diffusivity is substantially reduced ( $\chi_e < 0.1 \text{ m}^2 \text{ s}^{-1}$ ) and the transport is dominated by the ion channel which drops to neoclassical levels

TAB.1 FTU RECORD DISCHARGES

SHOT	B [T]	I [MA]	$\bar{n}$ [ $10^{20} \text{ m}^{-3}$ ]	T [keV]	n-yield [ $10^{13} \text{ s}^{-1}$ ]	$\tau_e$ [ms]	H <sub>89P</sub>	$n_0 T_0 \tau_e$ [ $10^{20} \text{ m}^{-3} \text{ K}$ ]
11612	6	0.7	2.1	1.2	0.2	75	1.5	0.4
12744	7	0.8	3.0	1.1	0.5	75	1.5	0.6
18598	8	1.2	4.0	1.4	1.3	80-100	1.4-1.7	0.6-1.0

. The achieved confinement time is above ITER-89P. The resulting values of the fusion figure of merit,  $n_{e0} E T_{i0}$ , are in the range of  $10^{20} \text{ m}^{-3} \text{ keV s}$  and are achieved in conditions where electron and ion temperatures are equal and  $Z_{\text{eff}}$  close to unity. The table shows the relevant parameters of pellet fuelled shots at various magnetic fields. An accurate density profile was not available for the 8T shot; the range in the table corresponds to the result of the kinetic

analysis and the confinement obtained from the equilibrium measurements, which overestimate the energy content.

In an attempt to heat and/or to stabilise  $m=1$  modes, effective coupling of LHCD to high density, high field plasmas;  $1.2 \times 10^{20} \text{m}^{-3}$ , 7.9T, 1.2 MA, 0.8 MW has been achieved. A 40% increase in neutron yield together with a 20 % drop in loop voltage and good confinement was observed with about 1 MW of LHCD power. In some cases,  $m=1$  modes were stabilised. At the very high density achieved during the multiple pellet phase, LHCD is not effective enough with the presently available power to really affect the plasma behaviour.

Several 1.6 MA discharges were obtained during the last week of FTU high performance operation. Pellet injection, up to three pellets, was studied. Some of the discharges were terminated by a disruption for reasons under investigation, likely linked to the lack of tuning of the operation with pellet injection. MHD activity which could be associated with high plasma current density operation ( $q_{\text{edge}}=2.5$ ) has not posed significant problems.

Steady neutron yield of  $10^{13} \text{n/s}$  was achieved in the post pellet phase, one of the highest achieved so far in FTU discharges. It confirms the trend indicating that performances of multiple pellet operation increase with increasing plasma current.

A new correlation reflectometer has been installed on FTU. Its results show a similar structure of turbulence spectra as that observed on other machines such as T10 (broadband, quasi coherent, low frequency). Pellet induced high confinement discharges show the three components in core turbulence and only the low frequency component in the periphery [7].

### **3. ECRH on the current ramp and with pellet injection**

The control of the current density radial profile can be a tool for reducing the level of turbulent fluctuations causing anomalous transport. The formation of transport barriers with flat or hollow current density profiles has indeed been shown in several tokamaks[8-14]. On FTU, the transport behaviour in these conditions has been investigated by heating the plasma with Electron Cyclotron Resonant Heating (ECRH) during fast current ramps. If the ramp rate of the plasma current is sufficiently fast, the skin effect drives the plasma current preferentially in the outer part of the discharge producing a non-monotonic current density radial profile. Moreover the detail of the plasma startup conditions, the impurity content and the gas feed can influence the shape of the current profile. In addition, during plasma current ramp-up sawteeth are absent, and the underlying heat transport mechanisms can be disclosed.

The FTU ECRH system allows to perform such an investigation at high magnetic field values ( $B=5.3\text{T}$ ) and high plasma density ( $n < 2.4 \times 10^{20} \text{m}^{-3}$ ). Power deposition by ECRH is well localised; this allows to check the radial temperature profile response to variations of the location of the resonant absorption radius, and to determine the influence of the electron free energy sources on turbulent heat transport. Furthermore, by changing the current ramp rate and the startup conditions a variety of current density profiles can be obtained, and the stability of the discharge is accordingly affected.

In the following figures, the electron temperature radial profile is shown at different times during the ECRH phase for two discharges with different location of the resonant absorption radius. No MHD activity was present during the profile evolution shown, so that the profile shape is governed by heat transport only. Very high central electron temperature values (up to 14keV at line average densities around  $0.4 \times 10^{20} \text{m}^{-3}$ ) have been achieved with central resonance. These are among the largest electron temperature values achieved so far in a tokamak. Since the electron distribution function inside the power deposition layer is non-maxwellian, the strong peaking of the radiation temperature is apparent and corresponds to a

nearly flat energy profile in that region, with an effective electron temperature about 70% of the maximum value. Electron heat transport is dominated by thermal diffusion as exemplified when off-axis resonance is used.

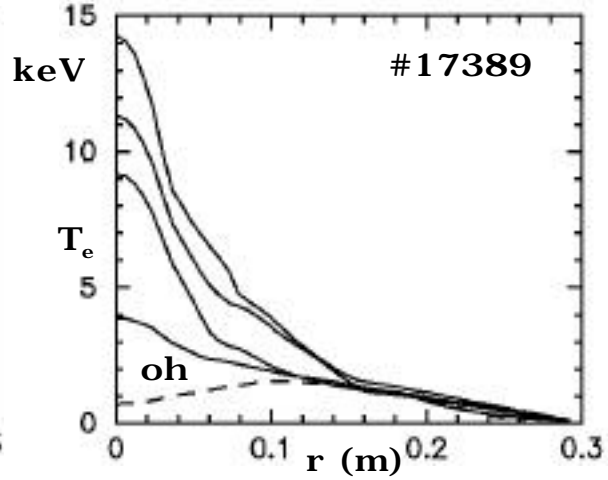
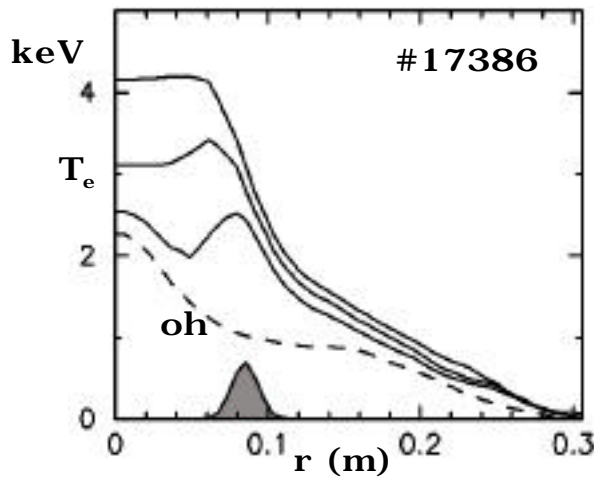


*FIG.2 Off-axis ECRH, 0.9 MW; electron temperature profiles before ECRH (dashed) and during ECRH, after 6, 11, 16 ms. Shaded area indicates the localization of the ECRH power*

*FIG.3 Central ECRH, 0.9 MW; electron temperature profiles before ECRH (dashed) and during ECRH, after 3, 8, 13, 23 ms*

The distortion of the electron distribution function is evident in the ECE spectra, measured by the Michelson interferometer, since both the third harmonic emission (which is nearly optically thick) and the downshifted second harmonic emission are well below the level implied by the central electron temperature. This result is consistent with the apparent peaking of the central electron temperature induced by a distortion of the bulk of the electron distribution function, as suggested by kinetic simulations[15]. Differently from other RF induced distortion, which typically produce energetic tails, in this case slope temperature of the electron energy distribution increases at energies below the thermal one. In order to measure the structure of the electron distribution function at low energies, an oblique ECE diagnostic was installed on FTU in collaboration with CIEMAT. It started operating at the end of the last experimental FTU campaign, and some preliminary data, with 400 kW of on-axis ECRH, have been obtained

Tearing modes and fast mixing events have been observed which can affect the transport properties in the internal region. Core confinement improvements have been observed when the minimum  $q$  was close to integer values and a stability window for MHD modes is expected.

The thermal diffusivity remains low even at extremely high values of the electron temperature gradient, i.e. in the presence of strong free energy sources which might drive turbulence[14,16]. This may be due to the beneficial effect of a flat/hollow current density profile on plasma turbulence theoretically predicted and experimentally observed also on other tokamaks. Note that improved confinement in other tokamaks was mainly achieved either at high  $T_i/T_e$  ratio or at low densities, whereas in FTU low thermal diffusivities are obtained at high density and high electron temperature.

The injection of high-speed solid deuterium pellets can improve the global energy confinement (by generating peaked pressure profiles), reduce ion transport to the neoclassical

level and suppress the sawtooth activity (generally by modifying the plasma current profile). Electron Cyclotron Resonance Heating has been used to increase the electron temperature in these very high density regimes, and to study the heat flux in the presence of a well-localised heat source[16].

As the central density is above the cut-off value ( $n_{Cr}=2.4 \times 10^{20} \text{ m}^{-3}$  at 140 GHz), optimum heating conditions are achieved with off-axis resonance. Central heating is affected by cutoff problems; as the ECRH power reaches the plasma centre, a strong density pump-out occurs, causes of which are being analysed. The cutoff is avoided by placing the resonance at  $r=a/3$ ; a moderate pump-out is observed in this case. Neoclassical ion heat transport and a subsequent improved global confinement can be transiently achieved in the optimised conditions. The duration of the improved regime is limited by the onset of an internal kink ( $m/n=1/1$ ) instability that leads to a decrease of the central density and a degradation of the ion confinement. A way to control the evolution of the current profile (with LHCD for instance) or to stabilise the kink mode will be needed to prolong the improved confinement phase.

#### 4. Formation of a reduced transport barrier during IBW injection

Ion Bernstein waves (IBW) have been proposed as a possible tool for pressure profile control in tokamaks. Theoretical calculations[17] show that, close to the absorption radius, IBW produce a sheared poloidal flow which, at sufficiently high power, can stabilize the

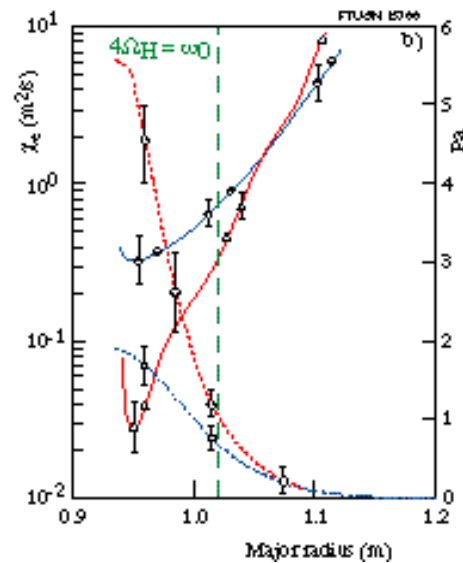
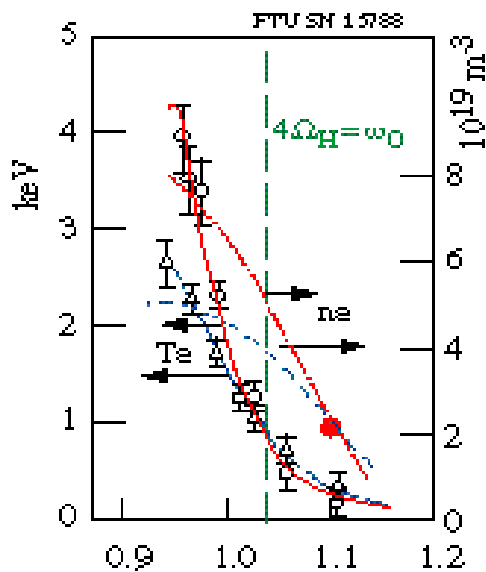


FIG.4 Temperature (scale on the left) and density (scale on the right) radial profile during the ohmic (blue) and during IBW heating (red) showing simultaneous peaking of both profiles close to the absorption radius (the vertical dashed line).

FIG.5 Thermal diffusivity (continuous line, scale on the left) and pressure radial profile (dotted line, scale on the right) before (blue) and during (red) IBW heating showing the reduction of the heat diffusivity in the part of the discharge.

turbulent fluctuations responsible for particle and heat transport. Previous results from PBX-M[18] gave some support to this possibility, whereas DIII-D[19] and TFTR[20] found no evidence of transport reduction. The IBW experiment on FTU is designed to minimize spurious effects, such as impurity release from the antenna, using a phased waveguide array

for coupling the RF power[21]. IBWs have been injected in FTU up to a coupled power of 0.35 MW (the present maximum available power) at the frequency of 433 MHz, corresponding to a RF power density of  $15 \text{ MW/m}^2$ . In order to have good core absorption and no peripheral damping, a hydrogen plasma at  $B = 7.9 \text{ T}$  was chosen. The 4th H ion-cyclotron harmonic resonant layer was located at about one third of the minor radius; thus, full IBW power absorption is expected at such a radius.

In these operating conditions, the IBW power injection produced a simultaneous increase of the central electron temperature (up to 2 keV) and peaking of the plasma density [22]. This result is shown in Fig. 4 and the corresponding increase in pressure profile is shown in Fig. 5. This figure also shows the electron thermal diffusivity profile obtained by the transport analysis. This analysis was performed using as an input in the JETTO code the experimentally determined electron temperature and density profiles, the equilibrium configuration, the radiation profile and the effective ion charge. The deposition profile expected from the linear theory and neoclassical resistivity were assumed. As a result, a reduced central electron diffusivity (up to an order of magnitude) is obtained during IBW injection, without any significant change of the ohmic power profile. The thermal diffusivity shows a reduction from the resonant layer to the axis. A local increase of the plasma pressure gradient is also observed, in agreement with the prediction of theoretical models for ExB sheared flow generation by IBW.

## 5. Synergy studies in combined injection of LH and Electron Cyclotron waves

Synergistic effects between Lower Hybrid (LH) and Electron cyclotron (EC) radio-frequency waves have been observed for the first time at a substantial power level in the FTU tokamak. Motivation for these studies was the prospect to combine their most interesting features, namely a high current drive (CD) efficiency for LH waves and a very localised, tuneable, and effective heating for EC waves. Indications of this interaction have been previously observed in other tokamaks [23]. Clear macroscopic effects have never been reported due to a series of limitations (transient scenarios, low plasma density and therefore electron collision time of the fast electrons larger than the radial diffusion time, low ECW absorption). The FTU experiment is equipped with more powerful RF sources ( $P_{\text{LH}}$  up to 0.9 MW at  $f_{\text{LH}}=8 \text{ GHz}$ ;  $P_{\text{EC}}$  up to 0.75 MW at  $f_{\text{EC}}=140 \text{ GHz}$ ), and relevant reactor characteristics: magnetic field of 7.2 T and central plasma density up to  $0.7 \times 10^{20} \text{ m}^{-3}$  in the reported domain of studies. In effect, very good current drive efficiency is achieved with LHCD alone at high magnetic field (7.2T) and full current drive has been obtained with an LH power of about 1 MW,  $n_{\text{eo}} = 0.5 \cdot 10^{20} \text{ m}^{-3}$  and  $I=400\text{kA}$ , the central electron temperature reaching 4 to 6 keV.

The synergy LHCD-EC is characterised by a substantial heating of the electrons at a magnetic field much higher than the resonant magnetic field for electron cyclotron resonance for which no heating is observed without LHCD. Energetic electron tails, which provide a substantial damping of EC waves, are enhanced and a consequent increase in electron temperature and current drive is observed. Up to 60 to 70% of EC power is estimated to be absorbed in this process. For  $B_{\text{T}}= 7.2 \text{ T}$ , the cold EC resonant value ( $B_{\text{T}}= 5 \text{ T}$ ) is well outside the FTU vessel. The EC waves (O-mode, outer perpendicular launch) cannot interact with the bulk electrons, whereas they can be absorbed by the suprathreshold electrons tail induced by LHCD, because the relativistic mass down-shifts the resonance frequency. Absorption of the EC power is evident for almost all conditions of density and current, as deduced from the fast EC emission, the hard X-ray (HXR) camera. Absorption can be as high as 70%, according to the probes detecting the escaping EC radiation. However macroscopic effects are observed

only when the fast electron tails are concentrated within a normalised radius  $r/a < 0.3$  and for  $n_e < 0.6 \times 10^{20} \text{ m}^{-3}$ . These conditions are likely to be due to the need of a sufficiently high suprathermal electrons density, which is presently limited by the available LH power. The EC power produces typically a slight increase of density, a clear drop in the loop voltage  $V_{\text{loop}}$ ,

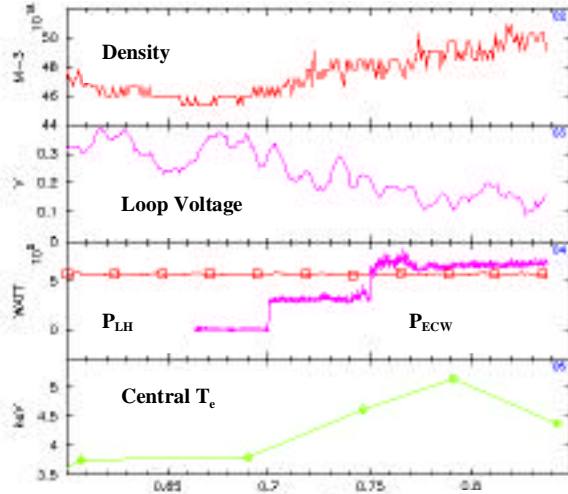


FIG.6 Time traces of density, loop-voltage, LH and ECRH power; central temperature during combined injection.

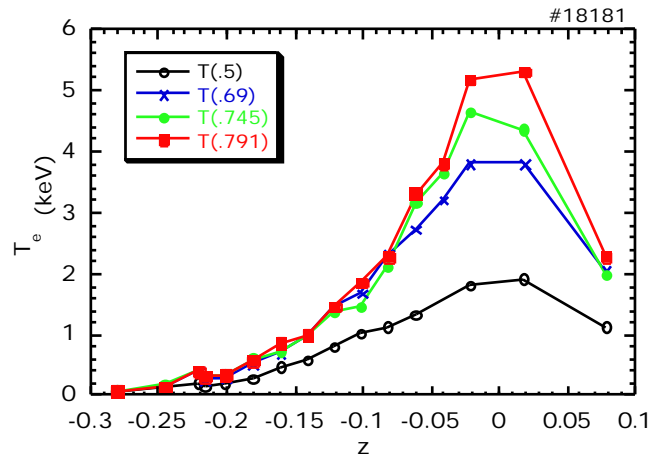


FIG.7 Thomson  $T_e(r)$  profile at different times: Ohmic phase (red), LH (0.6 MW) only (violet), LH+ECRH (0.6+0.35 MW: green; 0.6+0.7 MW: cyan)

and an increase larger than 1 keV in the central electron temperature (Fig6). The variation of the loop voltage,  $V_{\text{loop}}$ , is consistent with an extra driven current of about 10% (35-40 kA out of 350 kA total). Compared to the LH only phase, the electron temperature profile  $T_e(r)$  increases all over the region with  $r < 10 \text{ cm}$  ( $r/a < 0.3$ ), with  $T_{e0}$  doubling as the EC power doubles (Fig 7). The HXR data do not show large changes of the radial profile during the EC+LH phase, whereas the level of the signal is significantly increased. From the time evolution of the electron distribution function, estimated from HXR measurements, the EC perpendicular emission has been simulated in very good agreement with the measured spectra from the Michelson interferometer. A simulation [24] has been made including propagation of LH waves, build up of the fast electron population and down shifted damping of the EC waves. A multi-pass damping has to be included in order to reproduce the 70% absorption. The good agreement between HXR data and simulation indicates that the physics of the interaction EC waves – fast electrons is satisfactorily understood. This technique opens the prospect to use EC waves at a different field than the resonant field.

## 6. Tearing mode dynamics during ECRH

Tearing modes are systematically observed in FTU plasmas with high edge safety factor and low density. The increase of plasma pressure that can be induced by ECRH close to the plasma centre allows studying the dynamics of these modes as a function of the poloidal beta and to compare the results with the predictions based on neoclassical MHD models.



## 6.1 Neo-classical tearing mode dynamics

Two types of response of tearing modes to the effects of localised heating have been identified in FTU. The interpretation of these experimental results led for the first time to identify the detailed mechanism governing the rotation of toroidally coupled and uncoupled magnetic islands, associated to finite inertia and wall braking.

High power Electron Cyclotron Resonance Heating (ECRH) experiments have been performed on the FTU tokamak with the objective of controlling the MHD activity by fine adjustments of the position of the RF power absorbing layer. The fundamental resonance scheme at 140 GHz was used. A power  $P_{EC}=800$  kW was injected slightly off-axis in plasmas with major radius  $R_0=0.97$  m, minor radius  $a=0.27$  m, toroidal magnetic field  $B=5.6$  T, low plasma current ( $I_p$  350 kA), and high safety factor values ( $q_a \approx 6$ ). At these high  $q_a$  values, sawtooth relaxations are small or absent, while MHD oscillations with poloidal number  $m=2$  are observed in many cases. As a consequence of a moderate re-shaping of the current density profile and of a substantial increase of the plasma pressure induced by ECRH, the MHD oscillations are strongly amplified (Fig. 8), if the absorption radius  $r_{abs}$   $r_{q=1} < r_{q=2}$ . The oscillations are detected by a fast ECE multichannel polychromator, by an array of detectors for soft X-ray tomography and by a set of Mirnov coils. Cross-correlation analysis shows that the poloidal and toroidal periodicity of these fluctuations is  $m=2, n=1$ . In some cases, an  $m=1, n=1$  component is detected in the central region.

The oscillation frequency transiently increases as ECRH is applied, and then it slows down to locking while the area of profile flattening remains constant. The frequency evolution for a pure  $m=2, n=1$  mode (#15469) is shown in Fig. 9. In another case (#14979) an  $m=1$  mode is excited as a sideband by toroidal coupling to the  $m=2, n=1$  tearing mode.

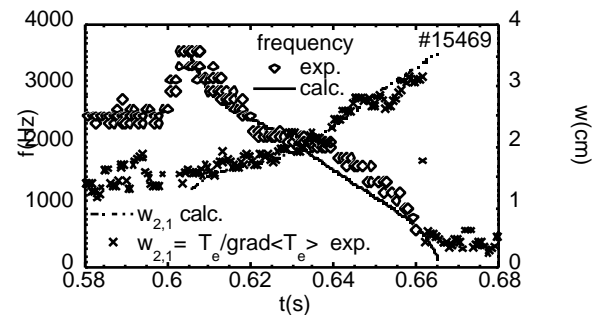
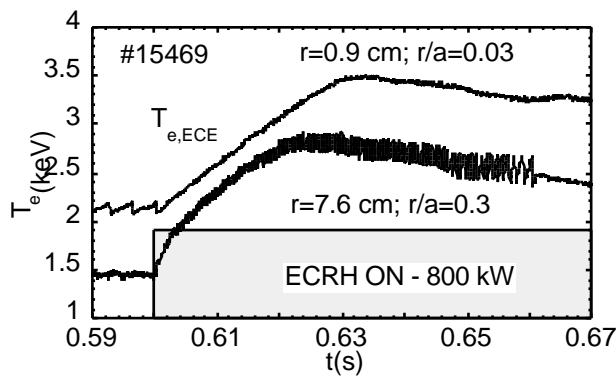


FIG.8  $T_e$  from two fast ECE channels (shot #15469), tuned close to the plasma center (top,  $r/a=0.03$ ) and to the position of maximum temperature oscillations (bottom,  $r/a=0.3$ )

FIG.9 Time evolution of the measured and calculated island width and rotation frequency for FTU shot #15469.

The frequency evolution of this case (Fig.10) is more complex than that of shot #15469 because here, as explained below there is a joint evolution of the  $m=1$  and  $m=2$  modes terminating with uncoupling of the  $m=1$  from the  $m=2$  while the latter locks to the wall. An interpretation of the observations and of the possible triggers of the modes can be given, through a suitable model for the evolution of the island width and rotation frequency. A non-linear dynamic model has been developed [25] extending the procedure introduced by Rutherford for large  $R/a$ , and resistive MHD ordering.

On the basis of the model presented in Ref. [25] the following interpretation can be given of the evolution of the rotation frequency shown in Fig.9 [26]. Before application of ECW power a marginally stable  $m=2$  mode is rotating at a constant frequency  $\omega_2$  corresponding to the local electron diamagnetic frequency  $\omega_{*m}/2 \sim 3\text{kHz}$ . The RF power input increases the pressure gradient and the frequency  $\omega_{*m}/2$  grows to 5 kHz while the mode is destabilized becoming a large rotating island. Subsequently ( $t > 0.62$ ) the island slows down in two stages. It can be stated that while the first stage with  $\omega_2 \propto W^{-1}$  (with  $W$  being the island width) corresponds to the *inertial effect* of the growing moment of inertia of the rotating island, the second stage is due to the wall eddy currents braking torque. This interpretation is supported by the results of the simulation shown in Fig. 9, where the calculated island width and mode frequency are compared with the measured ones. This shows clearly for *the first time* an inertial effect on rotation of a magnetic island, therefore clarifying their dynamic evolution.

The second important case of tearing mode frequency evolution is shown in Fig. 10 (shot #14979) together with the evolution reconstructed using the full system of coupled equations [26]. In shot 14979, two modes ( $m=1, n=1$ ) and ( $m=2, n=1$ ) are observed that rotate tightly coupled at the natural frequency of the  $m=2$  island,  $\omega_2/2 \sim 3\text{kHz}$ . When through wall braking the  $m=2, n=1$  mode is locked, the  $m=1$  keeps rotating uncoupled and eventually decays in amplitude. The numerical results of the model reproduce the essential features of the experimental observations; this confirms the role of inertia and wall interaction in determining the phase relations necessary for coupling.

## 6.2 Tearing mode stabilisation

The dynamics of TM strongly depends on the radial position of the absorbing layer, to the extent that the ( $m=2, n=1$ ) mode is fully suppressed if absorption occurs inside the magnetic island [27]. The width of the saturated island, as given by the amplitude of the corresponding flattened region of the  $T_e$  profile, is  $w \sim 3 \text{ cm} = 0.1a$ , which is comparable to the size of the EC power deposition profile  $w_{\text{abs}} = 2.5 \text{ cm}$ . Fine tuning of the absorption position with respect to the island, necessary for TM stabilisation, is achieved by steering the EC beams [28] and not by changing the toroidal magnetic field, which represents a step forward towards the active control and suppression of TM by EC waves.

Poloidal localisation of the absorption is as important as well. In fact, if the island is locked to the walls, in a position unfavourable for stabilisation, ECRH has no effect. In order to be suppressed, the island must rotate, allowing absorption at the O-point at each turn. Stabilisation is therefore achieved by smoothing out the  $m$ -order current density distortion on the resonant surface, and not by a local flattening of  $J(r)$  and the consequent reduction of the destabilising  $\omega'$  term. This is also consistent with the low power threshold necessary to achieve stabilisation, which is found to be  $P_{\text{ECRH}} \sim 0.15P_{\text{OH}}$ . If a change in the magnetic shear around  $r_{q=2}$  would be the origin for TM stabilisation, as for the case of sawteeth stabilisation, a power in the order of the ohmic one would likely be needed.

Stabilisation occurs even in the presence of a coupled ( $m=1, n=1$ ) mode, which vanishes a few ms after the suppression of the driving ( $m=2, n=1$ ) mode. Since the presence of coupled modes contributes to mode dynamics, in reactor applications for NTM stabilisation their presence shall be carefully considered both for adjusting the necessary power level, and for identifying the main driving mode, the first to be stabilised.

Stabilisation is achieved by ECRH, with perpendicular launch of the EC waves from the low field side. Experiments performed with ECCD, co and counter driven with respect to the ohmic current, and located at the same radial position as for pure ECRH, have shown no

difference in the stabilising effect. The negligible role of ECCD with respect to ECRH is due, in the cases considered, to the modest current drive efficiency in the relatively low  $T_e$  values at the absorption position. At the much higher temperatures expected in fusion plasmas where NTM stabilisation is required, the ECCD contribution should become dominant over ECRH.

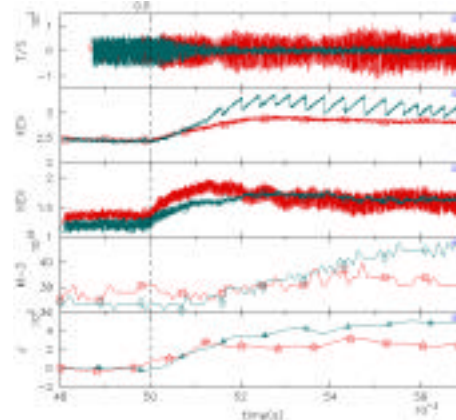
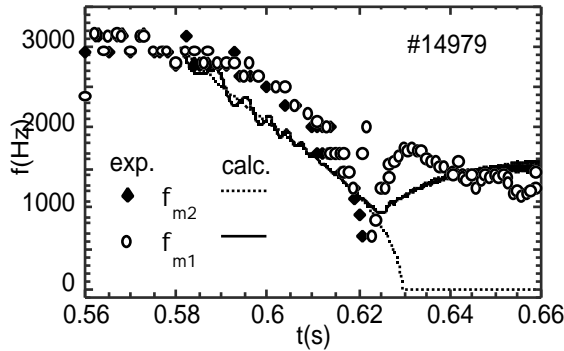


*FIG.10 Time evolution of the measured and calculated frequencies of fluctuations with  $m=1$  and  $m=2$  poloidal mode numbers for FTU shot #14979*

*FIG.11 Time traces of poloidal magnetic field fluctuations, central and half radius electron temperature, electron density and stored energy increase in two cases with and without stabilization*

After TM stabilisation, core confinement of both energy and particles is strongly enhanced. The peaking of the profiles following TM suppression may lead to the development of standard sawteeth, which in turn determine profiles no more unstable with respect to  $(m=2, n=1)$  tearing mode. It may happen, therefore, that  $(m=2, n=1)$  mode does not re-appear after removal of the stabilising EC power.

## 7. Impurity transport studies

Impurity transport and temperature effects have been studied at FTU, by means of mid – high Z elements (Fe, Ge, Mo, W), for high temperature ECRH heated plasmas. These experiments have been performed in collaboration with the Johns Hopkins University (JHU) and the Lawrence Livermore National Laboratory (LLNL). Medium-high Z elements have the advantage not to be fully ionised even at very high electron temperature (tens of keV) and to exhibit a large variety of soft X and VUV emissions very sensitive to the local plasma properties like temperature, non thermal effects, turbulence, changes of transport properties and so on [29]. X-ray emissions (L-shell) of intrinsic Mo in the core, heated by ECRH power at about 8 keV during the current ramp up with a magnetic shear still negative or zero, revealed a negligible impurity transport and a central impurity peaking [30].

## 8. Future plans

FTU will resume operation at the beginning of 2001. The reinstallation of the second LH launcher will allow to double the power available to the plasma. A multi-junction will replace one of the grills to test the feasibility of this coupling scheme for FTU plasmas. The

IBW power capability will be upgraded by inserting a second launcher which should bring the total available power up to 0.7MW. A boronisation system will be installed at the end of the present shut-down to improve the wall conditioning capability.

The modifications of FTU to allow the investigation of D-shaped plasmas (up to a plasma current of 0.45MA for single null operation) has been proposed and might start during the year 2002.

## References

- [1] CIRANT, S., et al., Proc. 10th Joint Workshop on ECE and ECRH, T. Donne' and Toon Verhoeven Editors, 369 (1997).
- [2] GREENWALD, M. et al. Phys. Rev. Lett. **53** (1984) 352
- [3] JET Team, Proc. 12<sup>th</sup> IAEA Conference, Nice 1988, IAEA (1989) Vol.1 p.215
- [4] Tore Supra Team, private communication
- [5] KAUFMANN, M., et al., Nucl. Fusion **28**, (1988) 827
- [6] FRIGIONE D. et al., Proc. 24th EPS, Berchtesgaden 1997, vol. 3 p 1177.
- [7] VERSHKOV, V. in preparation
- [8] LEVINTON, F. M. et al., Phys. Rev. Lett. **75**, (1995) 4417
- [9] STRAIT, E.J. et al. Phys. Rev. Lett. **75**, (1995) 4421.
- [10] JONES, T. T. C. and the JET Team, Phys. Plasmas **4**, (1997)1725
- [11] FUJITA, T. et al., Phys. Rev. Lett. **78**, (1997) 237
- [12] LITAUDON, X. et al., Plasma Phys. Contr. Fusion **38**, (1996)1603
- [13] GUNTER, S. et al., Phys. Rev. Lett. **84**, (2000) 3097
- [14] BURATTI, P. et al., Phys. Rev. Lett. **82** (1999) 560
- [15] KRIVENSKI, V., Proceedings of the 26<sup>th</sup> EPS Conference on Controlled Fusion and Plasma Physics, Maastricht, (EPS, Geneva 1999) **23J**, 385 (1999)
- [16] BRACCO, G., et al., Paper IAEA-EX6/3, this conference.
- [17] CRADDOCK, G., et al., Phys. Rev. Lett. **67** (1991) 1535.
- [18] LEBLANC, B., et al., Phys. Plasmas **2** (1995) 741.
- [19] PINSKER, R., et al., Proc. 8<sup>th</sup> Topical Conference on RF power in plasmas, Irvine 1989, (AIP, 1990), 314
- [20] ROGERS, J.C., et al., ., Proc. 12<sup>th</sup> Topical Conference on RF Power in plasmas, Savannah 1997, (AIP, 1997), 13
- [21] CESARIO, R. et al., and references therein, in 2<sup>nd</sup> Europhysics Topical Conference on Radio Frequency Heating and Current Drive of Fusion Devices, Brussels (Belgium) 1998, edited by J. Jaquinot, G. Van Oost, R.R. Weynants, European Physical Society, Brussels (Belgium) 1998, Vol. 22A, p. 65.
- [22] CESARIO, R. et al., submitted to Phys. Rev. Lett.
- [23] YAMAMOTO, et al. Phys. Rev. Lett. **58**, (1987) 2220
- [24] GIRUZZI, G. et al. Nucl. Fusion **29**, (1989) 1381
- [25] COELHO, R., LAZZARO, E., *Proc. of Joint-Varenna-Lausanne Int. Workshop on Theory of Fusion Plasmas*, p. 395, SIF.,Ed. Compositori, Bologna, Italy, 1998
- [26] LAZZARO, E., et al. Phys. Rev. Lett. **84**, (2000) 6038
- [27] CIRANT, S., et al., this conference
- [28] BRUSCHI, A., et al., "ECRH antenna at 140 GHz on FTU tokamak", to be published on Fusion Engineering and Devices
- [29] FOURNIER, K.B. et al., Phys. Rev. E, **53**, (1996) 1
- [30] PACELLA, D. et al., Phys. Rev. E, **61**, 5 (2000) 5